Finding the Mechanism of Wave Energy Flux Damping in Solar Pores Using Numerical Simulations

Julia M. Riedl [1] Caitlin A. Gilchrist-Millar [2] Tom Van Doorsselaere [1] David B. Jess [2]

[1]Centre for mathematical Plasma Astrophysics (CmPA), Department of Mathematics, KU Leuven

[2]Astrophysics Research Centre, School of Mathematics and Physics, Queen's University Belfast

724326

Motivation & context

Observations of slow magnetoacoustic waves (Gilchrist-Millar et al., 2020) imply that solar pores are suitable wave guides. However, the wave energy flux is damped surprisingly fast with height.

What mechanism is responsible for the damping?

→ **Mimicking observations with 2D simulations to find the damping mechanism**

2D model and driver

For our simulations, we create a gravitationally stratified 2D magnetohydrostatic equilibrium atmosphere ranging from slightly below up to a few hundred kilometers above the photosphere. The model is allowed to settle down until the changes are negligible compared to the driver period.

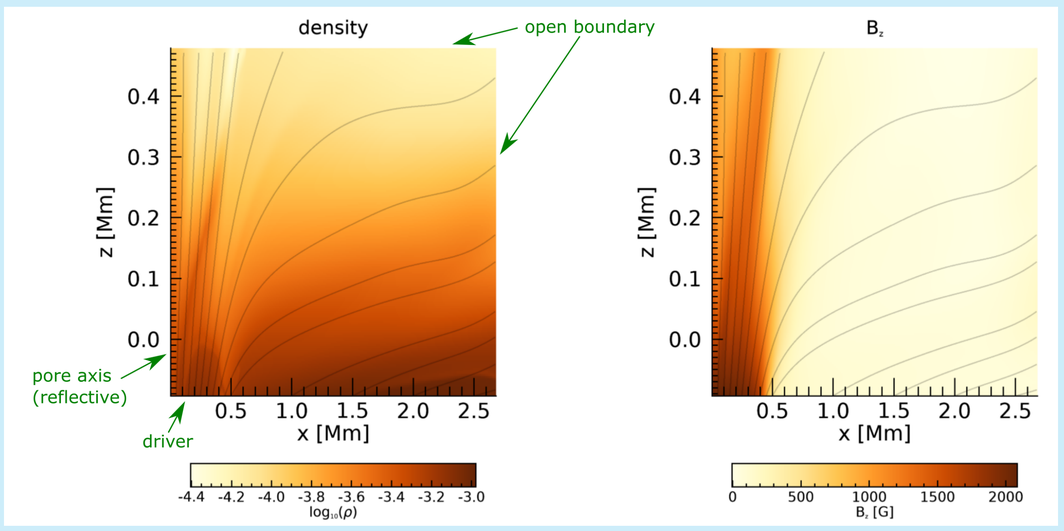

Figure 1: Density (left) and vertical magnetic field (right) of the model after settling down. The magnetic field lines are shown in grey. The solar pore is located at the left side of the plot, where the field lines are close to vertical.

The model is then perturbed by a velocity driver located at the bottom boundary

$$v_{z,\mathrm{driver}} = A \sin\left(\frac{2\pi}{T} t\right), \tag{1}$$

with $A = 160$m/s and $T = 30$s.
All simulations are conducted using the PLUTO code (Mignone et al., 2007).

Energy flux calculation

$$\vec{F} = -(\vec{v'} \times \vec{B'}) \times \vec{B'} + \left(\frac{\rho' v'^2}{2} + \rho' \Phi + \frac{\gamma}{\gamma - 1} p'\right) \vec{v'}, \tag{2}$$

where the primed variables denote perturbed variables.

Energy flux damping for a driver at full lower boundary

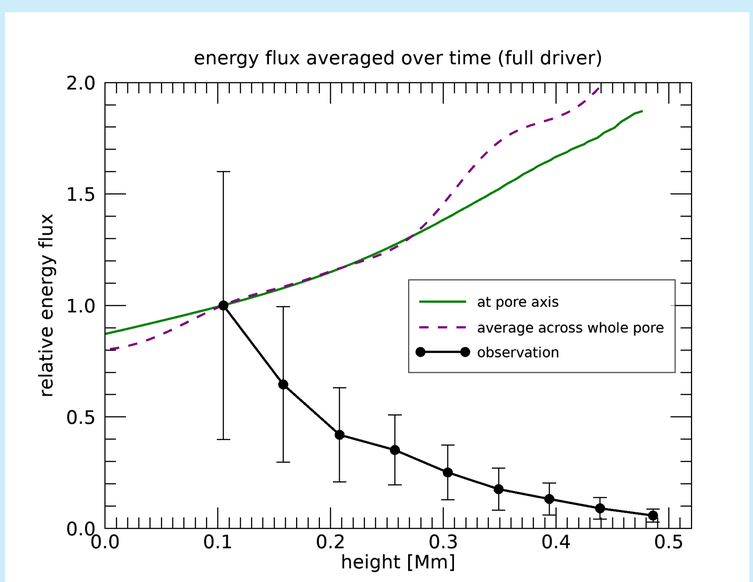

Figure 2: Time-averaged vertical energy flux for a driver located at the full bottom boundary, relative to the first observational data point.

For a driver covering the full bottom boundary the energy damping from the observations can not be reproduced. Adding viscosity, resistivity, or thermal conduction does not change the energy flux profile, since the effects are too small for such a narrow slice of atmosphere.

Energy flux damping for a localized driver

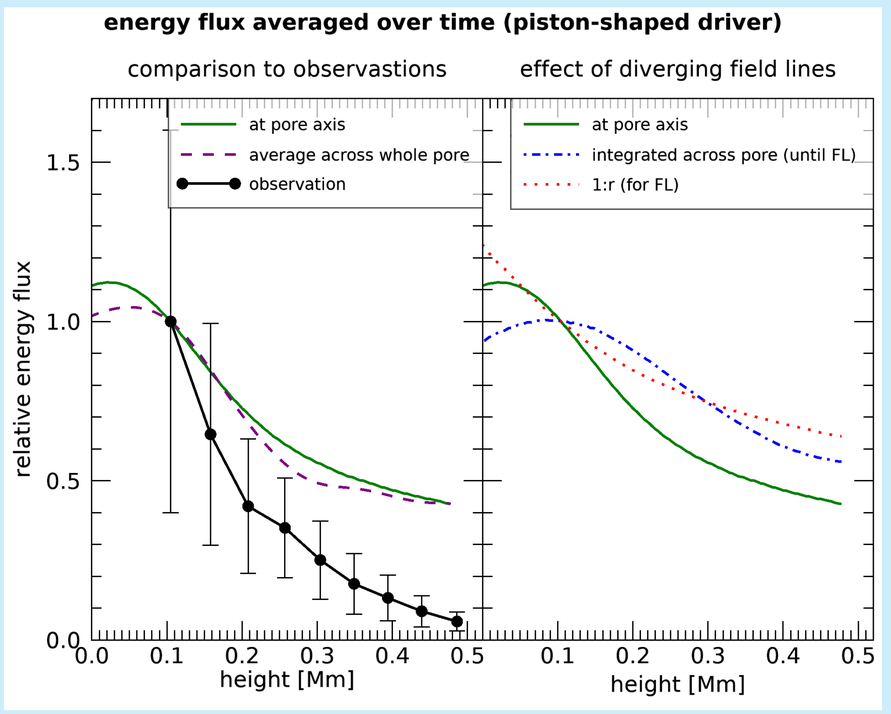

Figure 3: Time-averaged vertical energy flux for a driver located at $x \in [0, 0.2]$Mm, relative to the first observational data point.

A piston-shaped driver is used

$$v_{z,\mathrm{driver}} = \begin{cases} A \sin\left(\frac{2\pi}{T} t\right) & x \leq 0.2\mathrm{Mm} \\ 0 & x > 0.2\mathrm{Mm}. \end{cases}$$

This kind of localized driver can be justified by assuming the pore already starts at some point below the photosphere, acting as a wave guide.

The strong decrease in energy flux with height in the simulations seen in Figure 3 can be explained by the effects of two geometric mechanisms:

1. Geometric spreading of the waves due to diverging field lines and
2. MHD waves being able to propagate across field lines and therefore allowing them to leave the pore.

1. Geometric spreading

Since the field lines diverge, the same amount of wave energy flux is spread over greater areas, leading to a decrease in energy flux when following single field lines.

However, there must also be another mechanism at work, because

(a) energy flux decreases faster than $1/r$ (Figure 3, red dotted line)
(b) energy flux integrated across the pore from the axis to an arbitrary field line inside the driver location (FL) is not constant (Figure 3, blue dash-dotted line)

2. Waves propagating out of the pore

In a homogeneous plasma, the phase speed of slow and fast waves depends on the angle θ to the magnetic field direction

$$v_{f/s}(\theta) = \frac{\sqrt{v_s^2 + v_A^2}}{\sqrt{2}} \left[1 \pm \left(1 - \frac{4 v_c^2 \cos^2\theta}{v_s^2 + v_A^2}\right)^{1/2}\right]^{1/2}. \tag{3}$$

Taking that into account and tracing wave fronts assuming local homogeneity it can be seen that waves are allowed to leave the flux tube of the pore.

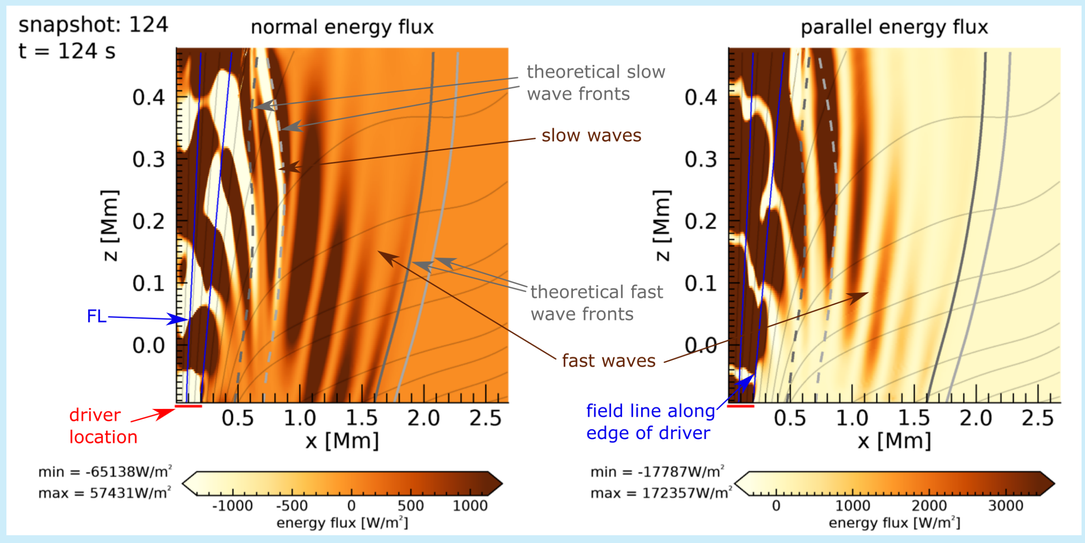

Figure 4: Normal (left) and parallel (right) energy flux components in respect to the magnetic field (saturated).